Supplementary information for

Defect-Engineered ZnO Nanoparticles Synthesized via Green Routes for Enhanced Solar Photocatalytic Activity

Delna Elizabeth Salu[a], Joshua Mathew James Lourd Raj[a], Krithikka Ashok Balamurugan Ramya[a], Vishwa Rohini Manivasagam[a], Jayanthi Eswaran[b], Rajakumar Kanthapazham[c], Ramkumar Vanaraj[d], Santhanaraj Daniel[a]

[a]Department of Chemistry

Loyola College,

Chennai 600 034

Tamil Nadu

India

[b]Department of Chemistry,

Kongunadu Arts and Science College,

Coimbatore - 641029, Tamilnadu, India

[c]Nanotechnology Research & Education Centre

South Ural State University,

Chelyabinsk - 454080,

Russia

[d]Department of Chemical Engineering,

Yeungnam University,

Gyeongbuk 38541,

Republic of Korea.

Corresponding authors

Prof. Santhanaraj Daniel [a**],

Phone: 7092053305

santhanaraj@loyolacollege.edu

Ramkumar Vanaraj[b]*

srirams27@gmail.com

Phone: 9842407059

Characterization of the catalysts

The particle size distribution and zeta potential of the synthesized ZnO nanoparticles were measured using a Malvern Zetasizer Nano ZS-90 instrument (Malvern Instruments Ltd., UK). The measurements were carried out at 25 °C using deionized water as the dispersing medium**.** The optical absorption properties of the ZnO samples were examined using a UV-Vis diffuse reflectance spectrophotometer in the wavelength range of 200-800 nm, with $BaSO_4$ serving as the non-absorbing reference standard. The spectra were recorded at room temperature, and the reflectance data were converted to absorbance using the Kubelka–Munk function to estimate the optical band-gap energy. The electron paramagnetic resonance (EPR) spectra of the ZnO samples were recorded using a BRUKER BIOSPIN EMX Plus X-band spectrometer (Germany) operated at room temperature. A microwave frequency of approximately 9.4 GHz was used, and the magnetic field was swept over an appropriate range to detect paramagnetic defect centers. The instrument was calibrated using the standard 2,2-diphenyl-1-picrylhydrazyl (DPPH). The surface chemical composition and oxidation states of the elements were analyzed using a Thermo Scientific ESCALAB 250Xi Base System equipped with UPS and XPS image mapping capabilities. The system was operated with an XR6 micro-focused monochromator employing Al Kα radiation (hν = 1486.6 eV) as the excitation source.

Table S1: Reported phytochemical composition and antioxidant activities of *Averrhoa bilimbi* and *Brassica oleracea* extracts. Values are expressed as gallic acid equivalents (GAE) or quercetin equivalents (QE), where applicable.

Plant species/ part	Solvent/ method	Total phenolic content (TPC)	Total flavonoid content (TFC)	Major identified compounds	Antioxidant / radical scavenging activity	Ref.
Brassica oleracea var. botrytis (cauliflower)	Ethanolic extract	165 µg GAE g^{-1}	348 µg QE g^{-1}	Catechin, Quercetin, Kaempferol	---	[1]
Averrhoa bilimbi (fruit)	Methanolic extract	209.25 mg GAE g^{-1}	---	Hexadecanoic acid, Squalene, Erucic acid, Oleic acid, 5-Hydroxymethylfurfural	NO-scavenging IC_{50} = 108.1 µg mL^{-1}	[2]
Averrhoa bilimbi (fruit)	Ultrasound-assisted conventional extraction (UACE)	---	851 ± 25 mg kg^{-1}	Myricetin (336 ± 15 mg kg^{-1}), Luteolin (231 ± 18 mg kg^{-1})	Superoxide-radical IC_{50} = 73 µg mL^{-1}; Reducing power = BHT	[3]

Table S2: Summary of synthesis parameters for ZnO nanoparticles prepared using bilimbi fruit and cauliflower leaf extracts.

Catalysts	Plant Extract	Extract: Precursor Volume Ratio (v/v)	Zinc Precursor	pH (adjusted with NaOH)	Reaction Temperature (°C)	Ageing/ Reaction Time	Drying Condition	Calcination Condition
$ZnO(B_1)$	Bilimbi fruit extract	1: 9	$Zn(CH_3COO)_2 \cdot 2H_2O$	8	25	1 h	60-70 °C, 3 h	500 °C, 3 h
$ZnO(C_1)$	Cauliflower leaf extract	1: 9	$Zn(CH_3COO)_2 \cdot 2H_2O$	8	25	1 h	60-70 °C, 3 h	500 °C, 3 h

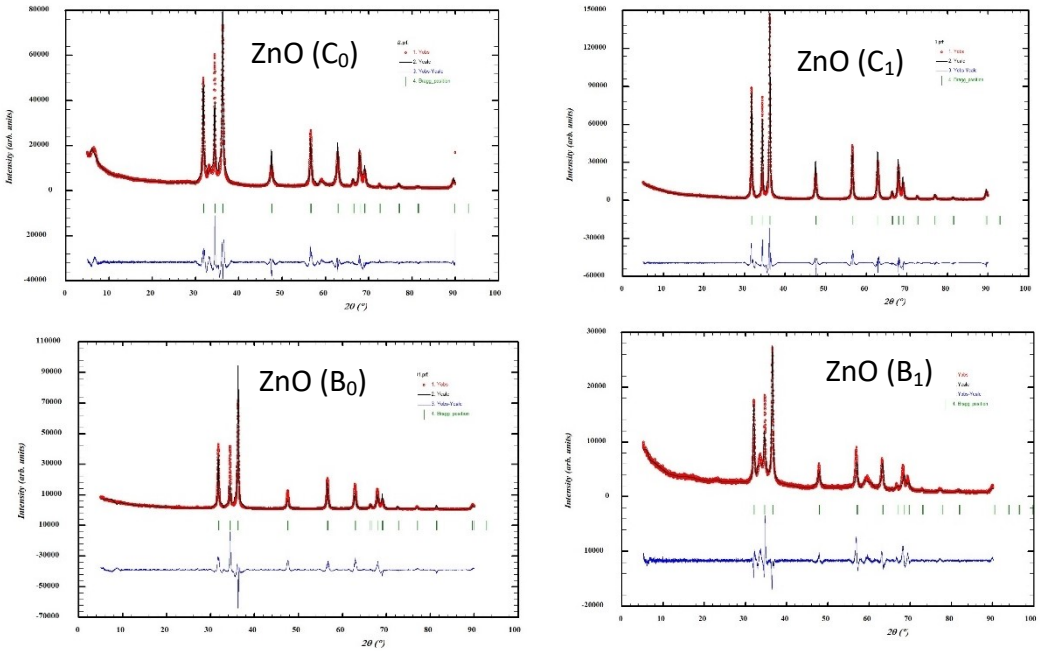

Figure S1: Rietveld refinement profile of XRD data of ZnO(C_0); ZnO (C_1); ZnO(B_0) and ZnO(B_1) catalysts. (*Averrhoa bilimbi* (ZnO B_0 and B_1) and cauliflower (ZnO C_0 and C_1), Before and after calcination.

1. Determination of crystallite size using Scherrer equation:

Table S1 displays the extracted parameters from the X-ray diffraction (XRD) profile, including 2θ values and Full-Width at Half Maximum (FWHM), while using Equation (1), the average crystallite size of the synthesized ZnO nanoparticles was reported:

$$D = \frac{K\lambda}{\beta_{hkl} Cos\theta_{hkl}} \quad \textbf{(1)}$$

Where D is the average crystallite size (nm), K is the shape factor (~ 0.9 for ZnO), λ is the wavelength of X-rays (1.540 x 10^{-10} m), β_{hkl} is the Full width at half maximum intensity (FWHM, in radians), and θ_{hkl} is the diffraction angle in radians

Table S3: Crystallographic parameters of the synthesized ZnO nanoparticles extracted from its XRD profile.

Plane	2θ	θ	Cos θ	FWHM (β, deg)	FWHM (β, rad)	β Cos θ (rad)	D (nm)	ln(1/cos θ)	ln(β·cosθ)
(002)	34.3833	15.8672	0.9619	0.2441	0.0034	0.0033	41.8600	0.0388	-5.7101
(100)	31.7344	17.1917	0.9553	0.1974	0.0043	0.0041	34.0846	0.0457	-5.5046
(101)	36.2104	18.1052	0.9505	0.2736	0.0048	0.0045	30.5642	0.0508	-5.3956
(102)	47.4980	23.7490	0.9153	0.4220	0.0074	0.0067	20.5774	0.0885	-5.0000
(110)	56.5590	28.2795	0.8806	0.3090	0.0054	0.0047	29.2089	0.1271	-5.3502
(103)	62.8150	31.4075	0.8535	0.4040	0.0070	0.0060	23.0515	0.1584	-5.1135
(200)	66.3720	33.1860	0.8369	0.3760	0.0066	0.0055	25.2589	0.1781	-5.2050

(112)	67.9060	33.9530	0.8295	0.3890	0.0068	0.0056	24.6327	0.1869	-5.1798
(201)	69.0460	34.5230	0.8239	0.3990	0.0070	0.0057	24.1785	0.1937	-5.1612
(004)	72.5230	36.2615	0.8063	0.3460	0.0060	0.0049	28.4897	0.2153	-5.3253
(202)	76.9040	38.4520	0.7831	0.5000	0.0087	0.0068	20.2989	0.2445	-4.9863

2. Williamson-Hall analysis:

i) Uniform Deformation Model (UDM):

The W-H UDM method was employed, where it is assumed that the strain is uniform in all crystallographic directions. The average crystallite size and lattice strain were estimated based on Equation (2):

$$\beta_{hkl} Cos\theta_{hkl} = \frac{K\lambda}{D} + 4\varepsilon Sin\theta_{hkl} \quad (2)$$

Where, β_{hkl} is the Full width at half the maximum intensity (FWHM, in radians), θ_{hkl} is the diffraction angle in radians, K is the shape factor (~ 0.9 for ZnO), λ is the wavelength of X-rays (1.540 x 10^{-10} m), D is the average crystallite size (nm), and ε is the microstrain

- A graph with $\beta_{hkl} Cos\theta_{hkl}$ on the y-axis v/s $4Sin\theta$ on the x-axis was plotted (using the data as presented in Table S2), which yielded:

i. $Slope = microstrain\ (\varepsilon)$

ii. $$D = \frac{K\lambda}{y - intercept}$$

Table S4: Calculated UDM model data of synthesized ZnO nanoparticles (ZnO B_1).

Plane	2θ	θ	FWHM (β, deg)	FWHM (β, rad)	Cos θ (rad)	4 Sin θ (x)	β Cos θ (y)
(002)	34.3833	17.1917	0.2441	0.0043	0.9553	1.1823	0.0041
(100)	31.7344	15.8672	0.1974	0.0034	0.9619	1.0936	0.0033
(101)	36.2104	18.1052	0.2736	0.0048	0.9505	1.2431	0.0045
(102)	47.4980	23.7490	0.4220	0.0074	0.9153	1.6109	0.0067
(110)	56.5590	28.2795	0.3090	0.0054	0.8806	1.8951	0.0047
(103)	62.8150	31.4075	0.4040	0.0070	0.8535	2.0845	0.0060
(200)	66.3720	33.1860	0.3760	0.0066	0.8369	2.1894	0.0055
(112)	67.9060	33.9530	0.3890	0.0068	0.8295	2.2341	0.0056
(201)	69.0460	34.5230	0.3990	0.0070	0.8239	2.2669	0.0057
(004)	72.5230	36.2615	0.3460	0.0060	0.8063	2.3659	0.0049
(202)	76.9040	38.4520	0.5000	0.0087	0.7831	2.4874	0.0068

ii) **Uniform Stress Deformation Model (USDM):**

Incorporation of Hooke's law in the UDM model results in the USDM model of W-H analysis, where, using Equation (3), the average crystallite size, stress and strain of the synthesized ZnO nanoparticles were determined:

$$\beta_{hkl}Cos\theta_{hkl} = \frac{K\lambda}{D} + \frac{4\sigma Sin\theta_{hkl}}{E_{hkl}} \quad (3)$$

Where, β_{hkl} is the Full width at half the maximum intensity (FWHM, in radians), θ_{hkl} is the diffraction angle in radians, K is the shape factor (~ 0.9 for ZnO), λ is the wavelength of X-rays (1.540 x 10^{-10} m), D is the average crystallite size (nm), and σ is the stress

- A graph with $\beta_{hkl}Cos\theta_{hkl}$ on the y-axis v/s $4Sin\theta/E_{hkl}$ on the x-axis was plotted (using the data as presented in Table S3), which yielded:

i. $Slope = Stress\ (\sigma)$

ii. $$D = \frac{K\lambda}{y - intercept}$$

iii. $$Strain\ (\varepsilon) = \frac{\sigma}{E_{hkl}}$$

Where σ is the stress (TPa) and E_{hkl} is the Young's modulus (TPa) (Equation (4))

Table S5: Calculated USDM model data of synthesized ZnO nanoparticles (ZnO B_1).

Plane	2θ	θ	FWHM (β, deg)	FWHM (β, rad)	Cos θ (rad)	4 Sin θ (rad)	Ehkl (TPa)	$4Sin\theta/E_{hkl}$ (x)	β Cos θ (y)
(002)	34.3833	17.1917	0.2441	0.0043	0.9553	1.1823	0.1441	8.2050	0.0041
(100)	31.7344	15.8672	0.1974	0.0034	0.9619	1.0936	0.1273	8.5938	0.0033
(101)	36.2104	18.1052	0.2736	0.0048	0.9505	1.2431	0.0822	15.1263	0.0045
(102)	47.4980	23.7490	0.4220	0.0074	0.9153	1.6109	0.0788	20.4486	0.0067
(110)	56.5590	28.2795	0.3090	0.0054	0.8806	1.8951	0.1273	14.8916	0.0047
(103)	62.8150	31.4075	0.4040	0.0070	0.8535	2.0845	0.0904	23.0497	0.0060
(200)	66.3720	33.1860	0.3760	0.0066	0.8369	2.1894	0.1273	17.2046	0.0055
(112)	67.9060	33.9530	0.3890	0.0068	0.8295	2.2341	0.0781	28.5909	0.0056
(201)	69.0460	34.5230	0.3990	0.0070	0.8239	2.2669	0.1041	21.7782	0.0057
(004)	72.5230	36.2615	0.3460	0.0060	0.8063	2.3659	0.1441	16.4192	0.0049
(202)	76.9040	38.4520	0.5000	0.0087	0.7831	2.4874	0.0822	30.2689	0.0068

Young's modulus:

Young's modulus (E_{hkl}) of the synthesized ZnO nanoparticles was calculated from Equation (4) as (using the data as presented in Table S4):

$$E_{hkl} = \frac{[\,h^2 + \frac{(h+2k)^2}{3} + \left(\frac{al}{c}\right)^2]^2}{S_{11}\left(h^2 + \frac{(h+2k)^2}{3}\right) + S_{33}\left(\frac{al}{c}\right)^4 + (2S_{13} + S_{44})\left(h^2 + \frac{(h+2k)^2}{3}\right)\left(\frac{al}{c}\right)^2} \quad (4)$$

Where h,k,l are the Miller indices, a & c are the lattice constants (a = 3.25; c = 5.21), and S_{11}, S_{33}, S_{13}, S_{44} are the Elastic compliance values of hexagonal compounds, whose values used were:

S_{11} = 7.86 x 10^{-12} Pa

S_{33} = 6.94 x 10^{-12} Pa

S_{13} = 2.21 x 10^{-12} Pa

S_{44} = 2.36 x 10^{-12} Pa

Table S6: Calculated Young's modulus data of synthesized ZnO nanoparticles (ZnO B1).

h^2	$\frac{(h+2k)^2}{3}$	$\left(\frac{al}{c}\right)^2$	$\left(\frac{al}{c}\right)^4$	x	y	E_{hkl} (TPa)
0	0.0000	1.5565	2.4227	2.4227	16.8137	0.1441
1	0.0000	0.0000	0.0000	1.0000	7.8580	0.1273
1	0.0000	0.3891	0.1514	1.9297	23.4817	0.0822
1	0.0000	1.5565	2.4227	6.5357	82.9629	0.0788
1	0.0833	0.0000	0.0000	1.1736	9.2222	0.1273
1	0.0000	3.5021	12.2650	20.2693	224.1323	0.0904
4	0.0000	0.0000	0.0000	16.0000	125.7280	0.1273
1	0.0833	1.5565	2.4227	6.9688	89.1847	0.0781
4	0.0000	0.3891	0.1514	19.2644	185.0701	0.1041
0	0.0000	6.2260	38.7635	38.7635	269.0184	0.1441
4	0.0000	1.5565	2.4227	30.8748	375.7065	0.0822

Where x = $[\,h^2 + \frac{(h+2k)^2}{3} + \left(\frac{al}{c}\right)^2]^2$

y = $[S_{11}\left(h^2 + \frac{(h+2k)^2}{3}\right) + S_{33}\left(\frac{al}{c}\right)^4 + (2S_{13} + S_{44})\left(h^2 + \frac{(h+2k)^2}{3}\right)\left(\frac{al}{c}\right)^2]$

iii) <u>Uniform Deformation Energy Density Model:</u>

UDEDM model relates strain to energy density as (Equation (5)):

$$\beta_{hkl}Cos\theta_{hkl} = \frac{K\lambda}{D} + 4Sin\theta_{hkl}\left(\frac{2u}{E_{hkl}}\right)^{1/2} \quad (5)$$

Where, β_{hkl} is the Full width at half the maximum intensity (FWHM, in radians), θ_{hkl} is the diffraction angle in radians, K is the shape factor (~ 0.9 for ZnO), λ is the wavelength of X-rays (1.540 x 10^{-10} m), D is the average crystallite size (nm), σ is the stress, u is the energy density, and E_{hkl} is the Young's modulus (TPa)

- A graph with $\beta_{hkl}Cos\theta_{hkl}$ on the y-axis v/s $4Sin\theta \bullet (2/E_{hkl})^{1/2}$ on the x-axis was plotted (data as presented in Table S5), which yielded:

i. $u = (Slope)^2$

Where, u is the energy density (TPa x 10^9 = kJ/m^3)

ii. $D = \frac{K\lambda}{y - intercept}$

Where D is the average crystallite size (nm), K is the shape factor (~ 0.9 for ZnO), and λ is the wavelength of X-rays (1.540 x 10^{-10} m)

iii. $Strain\ (\varepsilon) = \left(\frac{2u}{E_{hkl}}\right)^{1/2}$

iv. $Stress\ (\sigma) = \sqrt{2uE_{hkl}}$

Table S7: Calculated UDEDM model data of synthesized ZnO nanoparticles (ZnO B1).

Plane	2θ	θ	FWHM (β, deg)	FWHM (β, rad)	Cos θ (rad)	4 Sin θ (rad)	Ehkl (TPa)	$(2/Ehkl)^{1/2}$	$4Sin\theta \bullet (2/E_{hkl})^{1/2}$ (x)	β Cos θ (y)
(002)	34.3833	17.1917	0.2441	0.0043	0.9553	1.1823	0.1441	3.7256	4.4047	0.0041
(100)	31.7344	15.8672	0.1974	0.0034	0.9619	1.0936	0.1273	3.9643	4.3355	0.0033
(101)	36.2104	18.1052	0.2736	0.0048	0.9505	1.2431	0.0822	4.9333	6.1323	0.0045
(102)	47.4980	23.7490	0.4220	0.0074	0.9153	1.6109	0.0788	5.0386	8.1168	0.0067
(110)	56.5590	28.2795	0.3090	0.0054	0.8806	1.8951	0.1273	3.9643	7.5128	0.0047
(103)	62.8150	31.4075	0.4040	0.0070	0.8535	2.0845	0.0904	4.7027	9.8027	0.0060
(200)	66.3720	33.1860	0.3760	0.0066	0.8369	2.1894	0.1273	3.9643	8.6797	0.0055
(112)	67.9060	33.9530	0.3890	0.0068	0.8295	2.2341	0.0781	5.0592	11.3025	0.0056
(201)	69.0460	34.5230	0.3990	0.0070	0.8239	2.2669	0.1041	4.3833	9.9368	0.0057
(004)	72.5230	36.2615	0.3460	0.0060	0.8063	2.3659	0.1441	3.7256	8.8143	0.0049
(202)	76.9040	38.4520	0.5000	0.0087	0.7831	2.4874	0.0822	4.9333	12.2713	0.0068

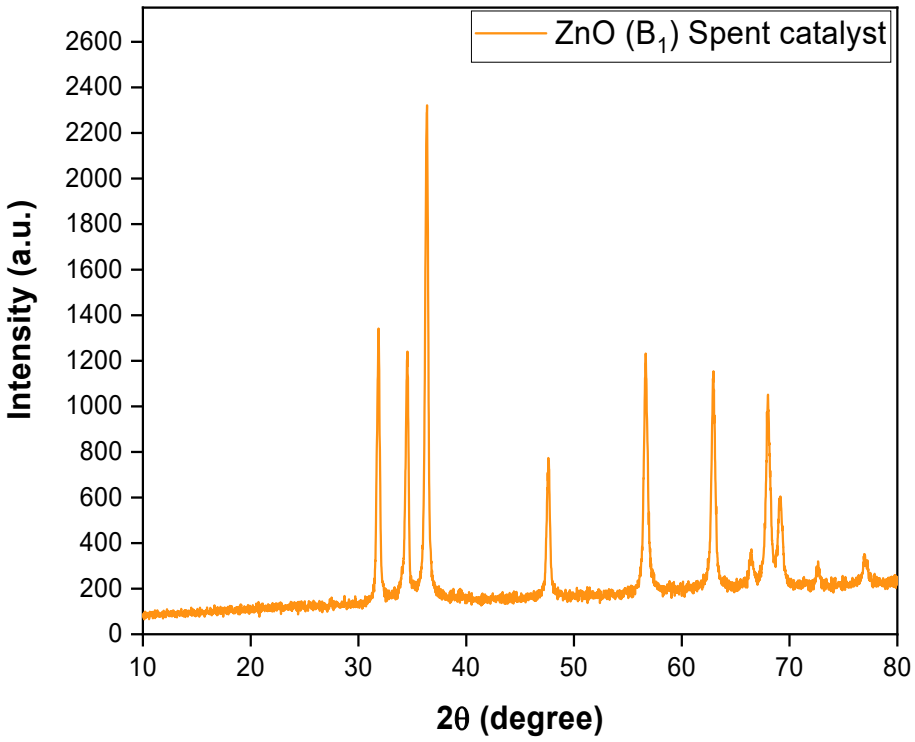

Figure S2: XRD pattern of spent catalyst ZnO (B_1).

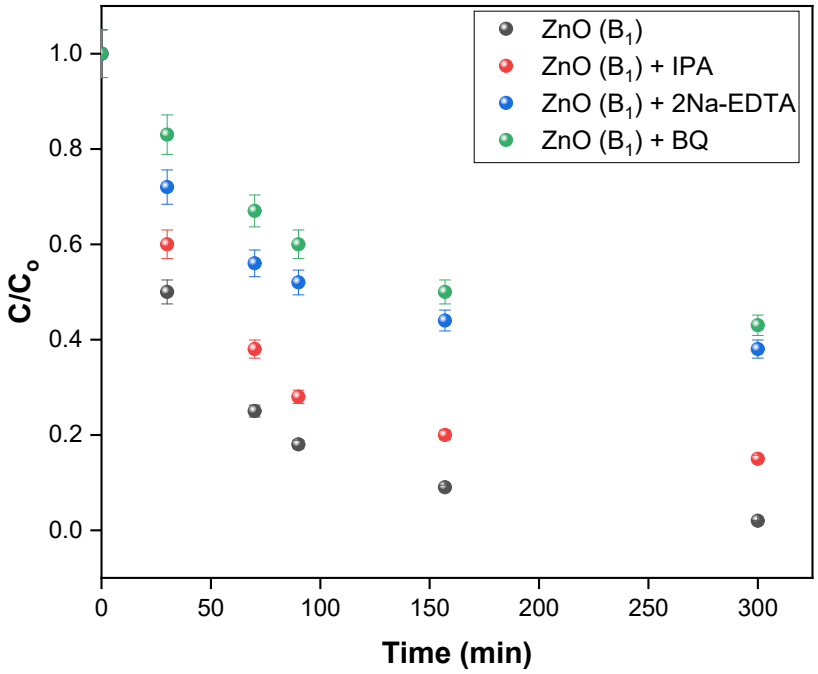

Figure S3: Photocatalytic degradation of MB by ZnO (B_1) in the presence of different scavengers (IPA, 2Na-EDTA and BQ).

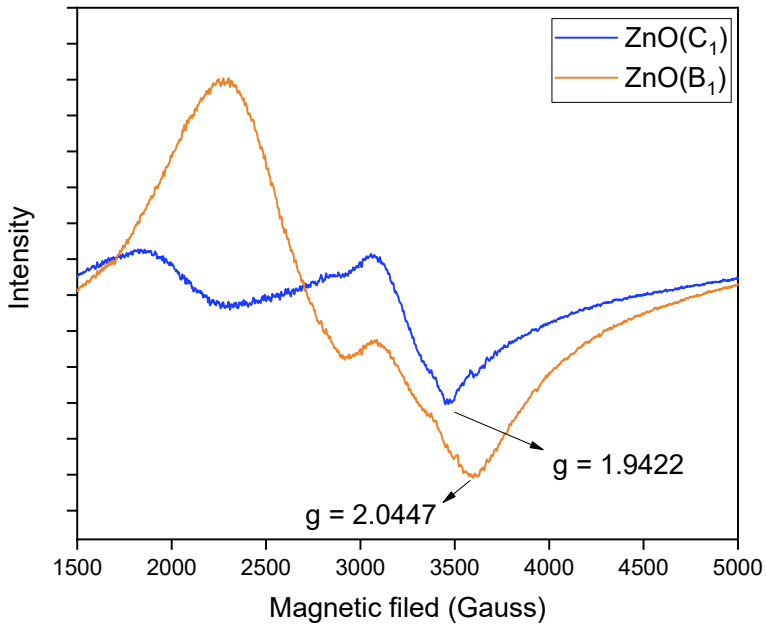

Figure S4: ESR spectra of calcined ZnO catalysts.

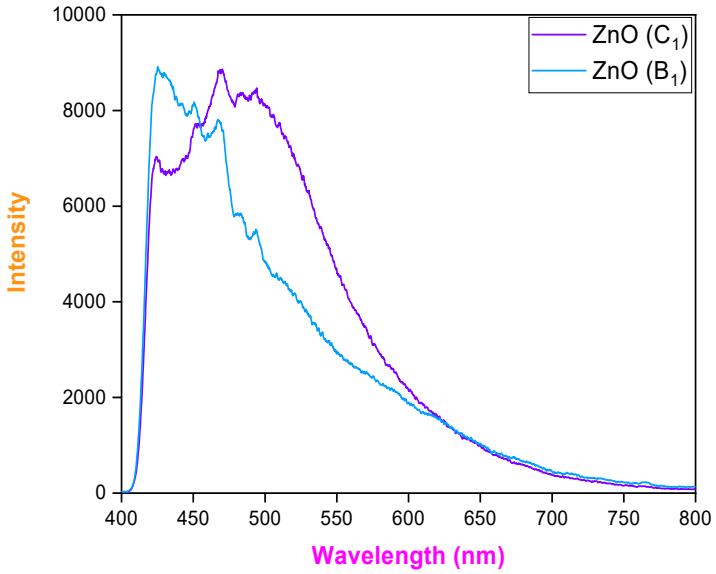

Figure S5: PL spectra of calcined catalysts (recorded using excitation wavelength at 380 nm with fixed PMT voltage at 700 V).

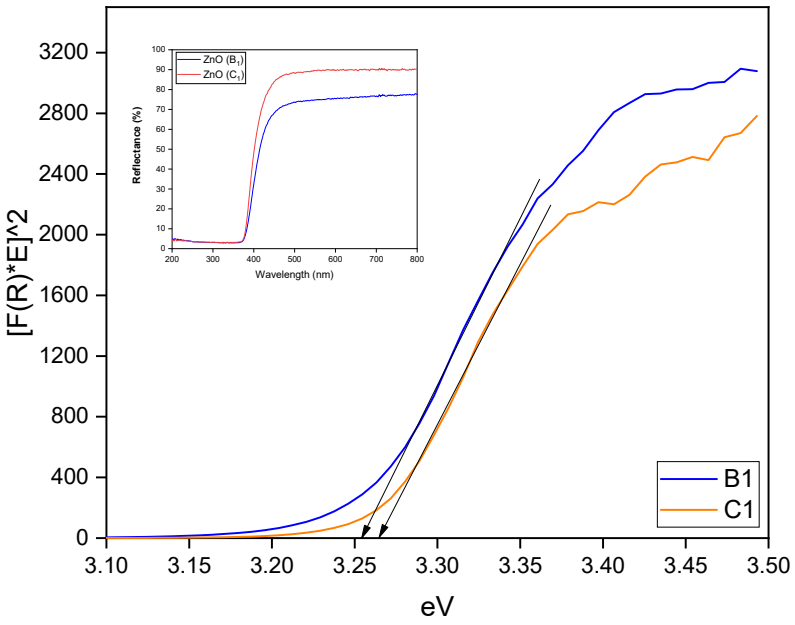

Figure S6: The energy band gap of ZnO (B_1) and ZnO (C_1) catalysts estimated by the extrapolation of the linear part of $[F(R)*E]^2$ versus eV plots (inserted UV-DRS spectra of samples).

References

[1] Rahman, M. M., Abdullah, A. T. M., Sharif, M., Jahan, S., Kabir, M. A., Motalab, M., & Khan, T. A. (2022). Relative evaluation of in-vitro antioxidant potential and phenolic constituents by HPLC-DAD of Brassica vegetables extracted in different solvents. *Heliyon*, *8*(10), e10838. https://doi.org/10.1016/j.heliyon.2022.e10838

[2] Suluvoy, J. K., & Grace, V. M. B. (2017). Phytochemical profile and free radical nitric oxide (NO) scavenging activity of Averrhoa bilimbi L. fruit extract. 3 Biotech, 7(1). https://doi.org/10.1007/s13205-017-0678-9

[3] Chau, T. P., Muthusamy, M., Chinnathambi, A., Alahmadi, T. A., & Kuppusamy, S. (2021). Optimization of extraction and quantification of Flavonoids from Averrhoa bilimbi fruits using RP-HPLC and its correlation between total flavonoids content against antimicrobial activity. Applied Nanoscience, 13(2), 1293–1300. https://doi.org/10.1007/s13204-021-02020-1